

# Parametric studies on punching shear behavior of RC flat slabs without shear reinforcement

Galal Elsamak\* and Sabry Fayed

Department of Civil Engineering, Faculty of Engineering, Kafrelsheikh University, Kafrelsheikh, Egypt

(Received June 12, 2019, Revised February 27, 2020, Accepted March 30, 2020)

**Abstract.** This paper proposed a numerical investigation based on finite elements analysis (FEA) in order to study the punching shear behavior of reinforced concrete (RC) flat slabs using ABAQUS and SAP2000 programs. Firstly, the concrete and the steel reinforcements were modeled by hexahedral 3D solid and linear elements respectively, and the nonlinearity of the used materials was considered. In order to validate this model, experimental results considered in literature were compared with the proposed FE model. After validation, a parametric study was performed. The parameters include the slab thickness, the flexure reinforcement ratios and the axial membrane loads. Then, to reduce the time of FEA, a simplified modelling using 3D layered shell element and shear hinge concept was also induced. The effect of the footings settlement was studied using the proposed simplified nonlinear model as a case study. Results of numerical models showed that increase of the slab thickness by 185.7% enhanced the ultimate load by 439.1%, accompanied with a brittle punching failure. The punching failure occurred in one of the tested specimens when the tensile reinforcement ratio increased more than 0.65% and the punching capacity improved with increasing the horizontal flexural reinforcement; it decreased by 30% with the settlement of the outer footings.

**Keywords:** RC flat slab; punching failure; finite element analysis; parametric analysis; simplified model; case study; footings settlement

## 1. Introduction

Flat-slab is the most recently used compared with the other types of slabs. Its architectural and economic features made it the top choice for all types of buildings. The most important advantages are the lack of beams, but this feature is the main reason of the failure by the punching shear. This type of failure is considered a brittle failure. It consists of shear diagonal cracks passing through the slab depth around the column. In the case of the rectangular columns consisted a frustum pyramid while a trenched cone occurred in case of the circular columns. There are many factors affecting the punching strength of slabs such as the column to slab aspect ratio, the concrete compressive strength, the top and bottom flexural reinforcement and the shear reinforcement.

The punching shear behavior of flat slabs were investigated experimentally by many researches. The slab thickness parameter was investigated by Birkle and Dilger (2008). The results showed that the slabs with a 230 mm thickness, without shear reinforcement, might not have an adequate safety if designed according to ACI 318-08 (2008). Alam *et al.* (2009) investigated the influence of the boundary restraint, the flexural reinforcing ratio and the slab thickness on punching shear behavior. It was found that as the flexural reinforcing ratio was enhanced from 0.5% to 1%, and the slab thickness was enhanced from 60 mm to 80 mm, the nominal shear capacity along the-critical perimeter

located at  $d/2$  from the column face increased. Guandalini *et al.* (2009) studied the impact of low flexural reinforcement ratios on the punching capacity of slab-column connections. It was found that the normalized punching shear strength decreased as the slab thickness increased and slabs with low flexural reinforcing ratios were found to fail in punching after an excessive yielding of the slab reinforcement. Sagaseta *et al.* (2011) also investigated the impact of the flexural reinforcement ratio on the punching capacity of the interior slab-column connections. Their investigation primarily focussed on investigating the behavior of slabs with different flexural reinforcing ratios in both orthogonal directions. It was found that slabs with non-axis symmetric reinforcing ratios did not have symmetric deflection responses in both orthogonal directions. It was also found that slabs with reinforcing ratios exceeding 0.75% failed brittlely in the punching shear. Lips *et al.* (2012) investigated the impact of the column size, slab thickness, shear reinforcement type and the amount of shear reinforcement on the punching shear behavior. It was found that if the column size increased, the punching capacity and the rotation at failure increased. Slab slenderness and its size were also found to impact the punching capacity, especially for slabs which failed due to the crushing of concrete struts. Einpaul *et al.* (2016) found that the shear capacity and flexural stiffness of the slabs decreased as the slab slenderness was increased and the nominal shear stresses along a critical perimeter located at  $d/2$  from the column face also decreased as the column diameter was increased. Saleh *et al.* (2018) investigated the punching shear behavior of high strength RC slab with and without shear strengthening reinforcement in the form of post-

\*Corresponding author, Assistant Professor  
E-mail: [jalaal\\_elSammak123@eng.kfs.edu.eg](mailto:jalaal_elSammak123@eng.kfs.edu.eg)

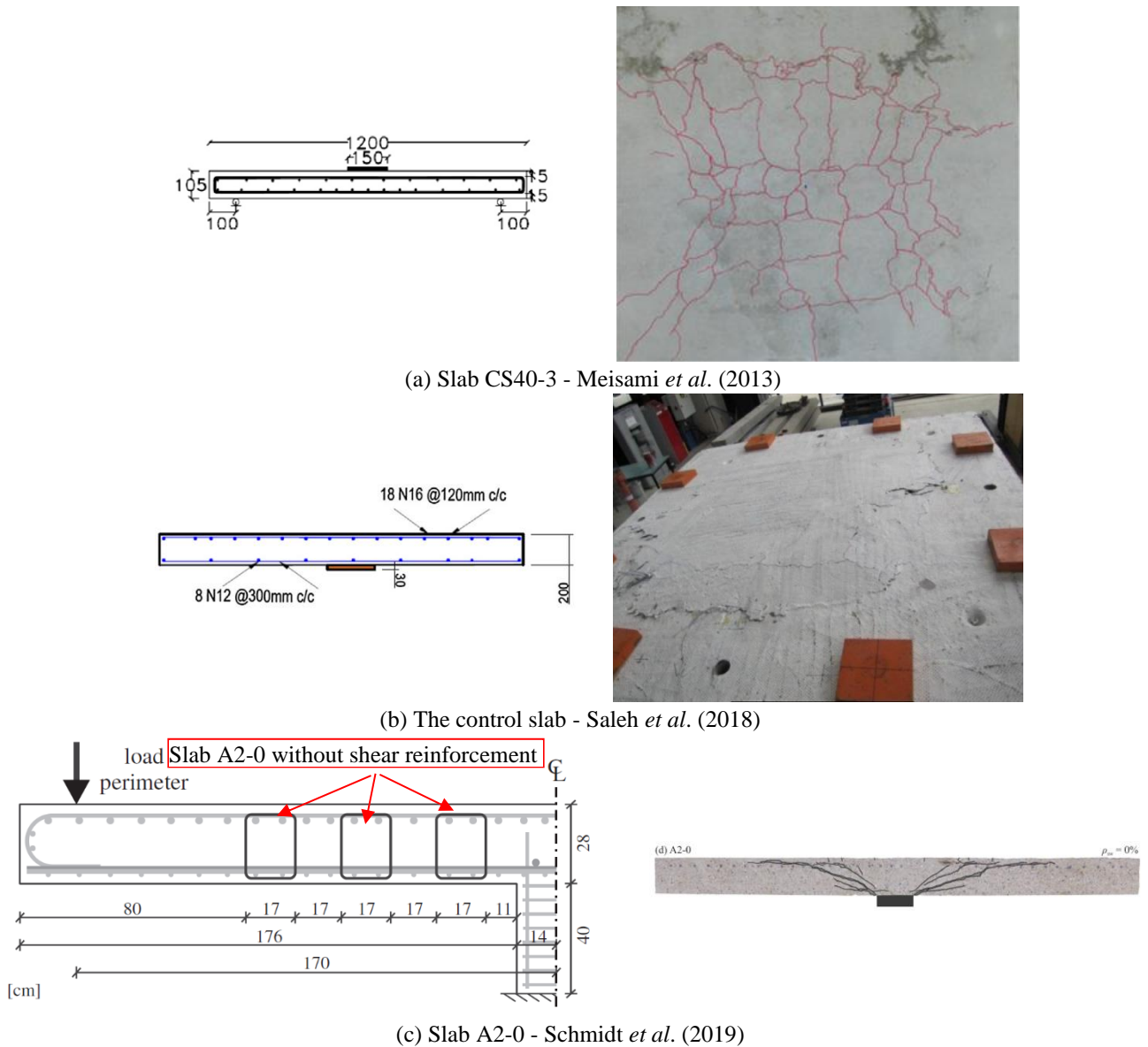


Fig. 1 Details and results of slabs that used to validate the slab numerical models

installed shear bolts. In the case of the un-strengthened slab, it was found that an increase of compressive strength of the slab without shear reinforcement from 25 MPa to 40 MPa led to an increase in the shear capacity of about 37%. Schmidt *et al.* (2019) studied the punching shear behavior of flat slabs with a varying amount of shear reinforcement, three systematic test series without and with stirrups as shear reinforcement were conducted. It was found that the punching failure of the specimens without or with very low amounts of shear reinforcement was directly triggered by the initial, relatively flat inclined shear crack.

The punching shear mechanism of RC slabs also was studied using numerical studies. Polak (2005) proposed a numerical investigation taking in consideration the out-of-plane shear response. Genikomsou and Polak (2014) induced a numerical study to model the RC slabs that failed in the punching shear and studied the collapse mechanism. The effect of flexure reinforcement, shear retention and fracture energy was proposed by Shu *et al.* (2016). Guan

(2009) induced an article in order to study the effect of the opening and its size on the shear punching of the slabs. Nonlinearity of the elements of RC slabs using multi-layered shell modelling were investigated and the FEA results were compared to the analytical and experimental results by Belletti *et al.* (2015). Ahsan and Zahura (2017) noted that the integrity reinforcement can increase the punching capacity as much as 19% in terms of force and 101% in terms of deformation.

There are not many studies about the effect of the flexural compression reinforcement and slab loading condition on the punching shear behavior of the flat slabs. This paper focused on developing FE models using ABAQUS programme (2014) and SAP2000 programme (2017). The parameters represent the slab thickness, the flexural reinforcement, either in tension or in compression, and the slab loading condition. Then to reduce the time of the FEA, a simplified model using SAP2000 was proposed. After that, a case study to show the effects of the settlement

Table 1 Material properties of slabs used to validate the slab numerical models

Test	Tensile steel reinforcement	Compressive steel reinforcement	Concrete $f_c$ (MPa)	Steel $f_y$ (MPa)
Meisami <i>et al.</i> (2013)	11 $\Phi$ 16; $\rho=2.20\%$	11 $\Phi$ 6; $\rho=0.35\%$	42.4	420
Saleh <i>et al.</i> (2018)	16N16; $\rho=1.30\%$	8N12; $\rho=0.86\%$	65.0	520
Schmidt <i>et al.</i> (2019)	34 $\Phi$ 20; $\rho=1.40\%$	38 $\Phi$ 10; $\rho=0.40\%$	34.9	529

of footings on the behavior of RC flat slab frame structures was performed.

## 2. The considered experimental studies

Meisami *et al.* (2013) proposed an experimental work to study the punching shear strengthening of RC flat slabs using CFRP rods under monotonic loading. Specimen CS40-3 was one from the control specimens and it was selected in the current research to validate the slab numerical models. The slab dimension was 1200×1200×105 mm. The flexure reinforcement in both directions of the slab was identical. The effective depth ( $d$ ) was 100 mm. An applied load was concentric with the slab centre. The four edges of the slab were simply supports and the static load was applied on the slab using loading plate of 150×150 mm to avoid the concrete crushing under the load. Rate of increasing the loads was carried out during the experiment using the displacement control.

Saleh *et al.* (2018) investigated the punching shear behavior of high strength RC slab with and without shear strengthening reinforcement in the form of post-installed shear bolts. Two large scale RC slabs representing an interior slab-column connection were tested. One slab was without shear reinforcement and it was used as a control slab. This slab was selected here in the current research to validate the slab numerical models. The control slab was square with side dimension of 2300 mm and 200 mm thick with an effective depth 154 mm. The punching load was applied from the bottom of the slab. The slab was supported on eight steel plates with dimensions 200 mm×200 mm×30 mm around the slab perimeter at a distance of 1125 mm from the centre of the slab. Monotonic load was applied to the centre of the slab using a steel bearing plate with dimensions 300 mm×300 mm×30 mm.

Schmidt *et al.* (2019) studied the punching shear behavior of flat slabs with a varying amount of shear reinforcement. Slab A2-0 was one from the control specimens and it was selected in the current research. The slab dimension was 3800×3800×280 mm with an effective depth of 225 mm. The square column stub had side dimensions of 280 mm was casted monolithically at the center of the flat slabs. The slab was loaded from above by means of 12 rigidly supported hydraulic jacks, which were equidistantly arranged in a circle with a radius of  $r=1700$  mm from the centre of the column.

The reinforcement and concrete properties for all slabs

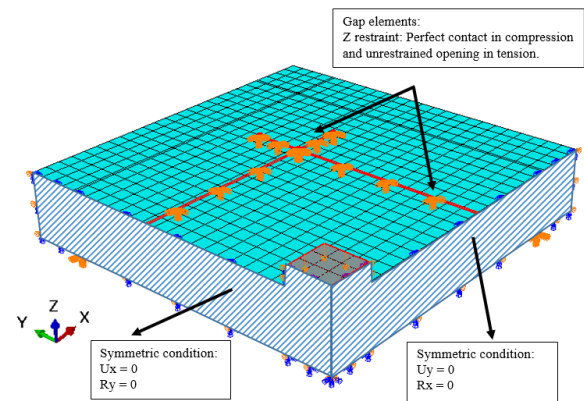


Fig. 2 Boundary conditions and loadings used in ABAQUS for specimen CS40-3

that used to validate the slab numerical models are listed in Table 1. Slabs layout and experimental failure modes were also shown in Fig. 1. It was noticed that all slabs failed under the brittle punching shear failure.

## 3. Finite element analysis using ABAQUS

The considered part of specimens simulates the zone of the negative bending moment around an internal column-slab connection up to the points of the contra flexure. Fig. 2 shows the loading condition of specimen CS40-3 which have two symmetric planes; XZ and YZ. So, one quarter of the slab was modelled to reduce the time of the analysis. Steel plates under the load and supports were connected with the concrete slab surface in order to avoid stress concentration at these locations. The concrete, loading plates and the supports were modelled using 8-nodes isoparametric brick elements (Type C3D8). The beam element (Type B31) with a 2-nodes linear displacement was adopted to model the reinforcing bars. The bond between the concrete and reinforcing bars was considered as a full bond. The surface between the concrete and the supports was modelled using gap elements (Type GAPUNI) without any horizontal restraint.

### 3.1 Modeling of materials

#### 3.1.1 Concrete

The concrete element was modelled using a damaged plasticity model. The dowel action and the bond slip of the rebar-concrete interaction were considered by introducing tension stiffening into the concrete softening behavior to simulate the load transfer across the cracks through the rebar. The curves of the stress versus the strain were evaluated by Eurocode 2 (2004) and these curves were considered in the current study to draw the stress-strain relationship for the concrete. For specimen CS40-3 as an example (as shown in Fig. 3), the curve of the concrete tension was fitted to the stress-displacement relationship while the curve of the concrete compression hardening was fitted to the stress-strain curve. The post-peak of the tension failure behavior of the concrete was specified using the

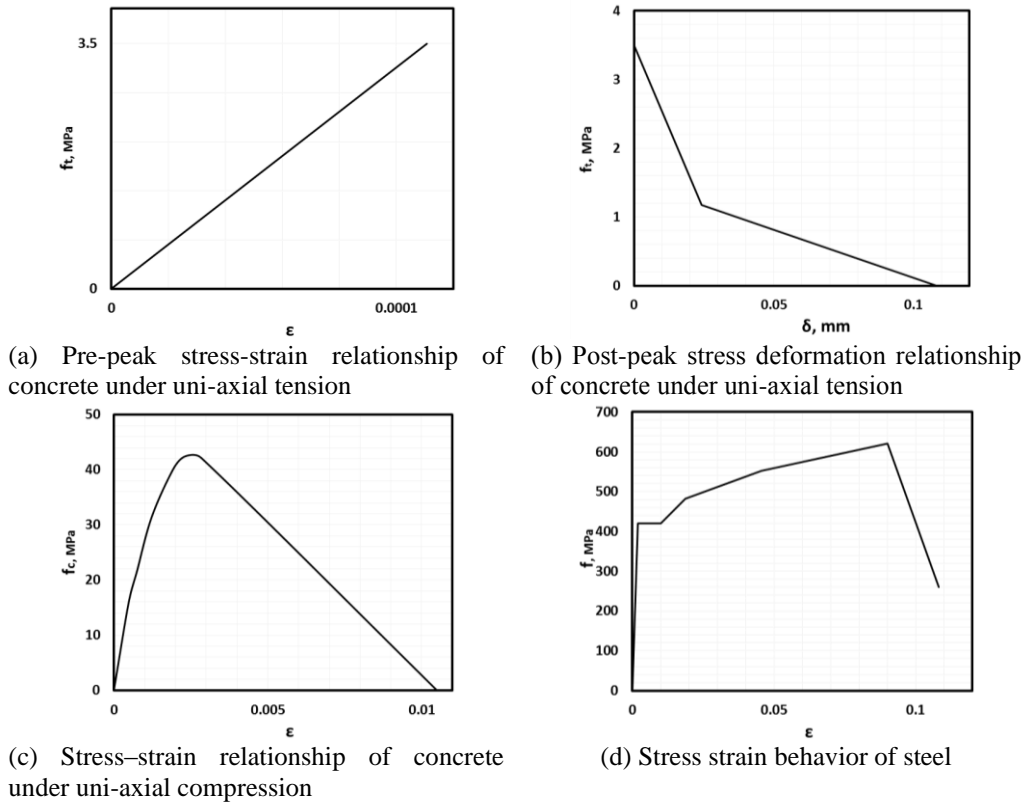


Fig. 3 Properties of concrete and steel materials for specimen CS40-3

Table 2 Parameters for concrete damaged plasticity model considered for specimen CS40-3

Dilation angle $\psi$	Eccentricity $\epsilon$	Viscosity $\mu$	Shape parameter $K_c$	Max. compression axial/biaxial
46°	0.1	Zero	0.67	1.16

method of fracture energy.  $G_f$  is the fracture energy of the model and is defined as the area under the curve of the softening. Poisson's ratio of 0.2 was taken for the concrete.

### 3.1.2 Reinforcing steel

Reinforcing steel material was commonly modelled either by nonlinear behaviour or bi-linear behavior. The bi-linear behavior was considered in recent study which were defined as linear elastic with strain hardening. The tension and compression behaviors were identical. To draw the stress strain curve for the reinforcing steel material, some items were needed such as: the yield stress ( $f_y$ ), the modulus of elasticity ( $E_s$ ), the ultimate stress  $f_u$  and the ultimate strain  $\epsilon_u$ . The Poisson's ratio of reinforcing steel material was taken by 0.3 and the stress strain curve of the reinforcing steel material is shown in Fig. 3(d) for specimen CS40-3.

### 3.2 Validation of the Model

For succinct modelling purpose and because the other two specimens will be modeled in the same way, only the specimen CS40-3 will be explained in detail.

For specimen CS40-3, the yield stress of the steel ( $f_y$ ) and the compressive strength of the concrete  $f_c$  were

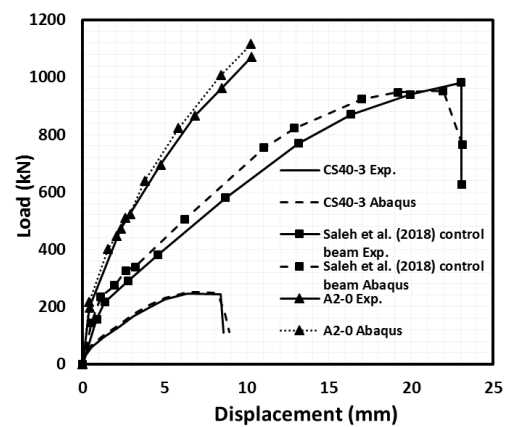


Fig. 4 Load-deflection curves of simulated slabs, obtained by experimental tests and ABAQUS simulation

Table 3 Model size for specimen CS40-3

Model	Number of solid elements	Number of beam elements	Total number of elements
CS40-3	3183	576	532

measured to be 420 and 42.4 MPa respectively. The modulus of elasticity of the concrete ( $E_c$ ) and the concrete tensile strength ( $f_{ct}$ ) were then calculated by Eurocode 2 (2004). The material properties for both the concrete and the steel bars are shown in Fig. 3. Table 2 shows the necessary items of the concrete model that they were used in the modeling. Also, the model size is listed in Table 3.

The load deflection behavior for all tested slabs was obtained experimentally and the comparisons between the

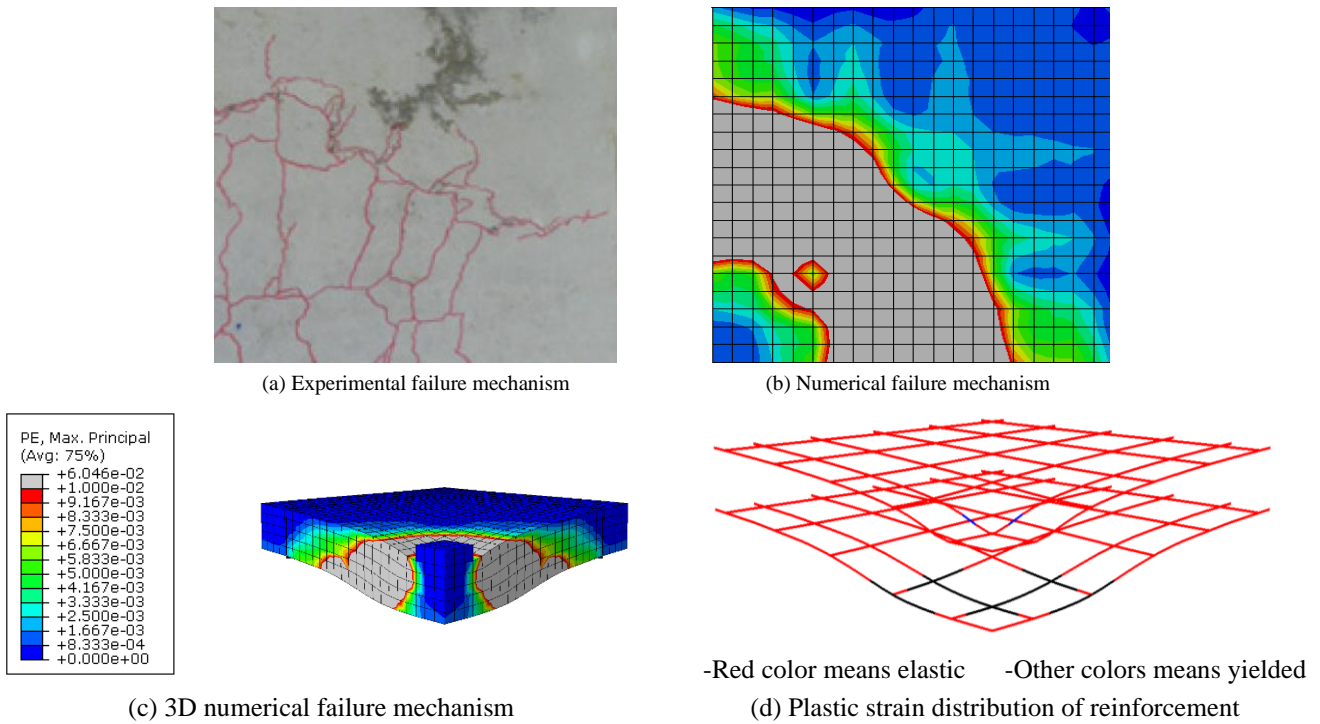


Fig. 5 Comparison between FE analysis and crack pattern from experimental test for specimen CS40-3

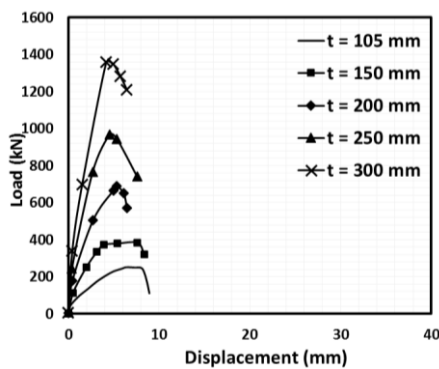


Fig. 6 Load-deflection curves for slabs with different thicknesses ( $t$ )

experimental and the numerical results for all slabs are shown in Fig. 4. The FEA results agreed well with the experimental results. The cracking pattern reported by Meisami *et al.* (2013) is illustrated in Fig. 5(a) is identical with the numerical failure pattern represented in Fig. 5(b) at ultimate load step. The specimen is failed by the punching shear. Punching shear cone of the simulation in the 3D failure mechanism was shown in Fig. 5(c). It is necessary to note that the plastic strain index shown in Fig. 5(c) was used for all plastic strain distributions in the recent study. The plastic strain distribution of the reinforcement is shown in Fig. 5(d).

As seen, the numerical modelling agreed well with the experimental results. The numerical curves and failure modes showed a good simulation of the behaviour of RC flat slabs.

#### 4. Parametric study using FEA

Table 4 Numerical results for slabs with various slab thicknesses

Specimen thickness ( $t$ )	Increase ratio of ( $t$ )%	$V_u$ (kN)	Increase ratio of $V_u$ %	$V_u/(\sqrt{f_c} \cdot b_0 \cdot d)$	$\Delta_u$ (mm)
105 mm	-	251.9	-	0.38	8.10
150 mm	42.8	383.8	52.36	0.34	7.50
200 mm	90.5	688.3	173.24	0.39	5.20
250 mm	138	967.2	283.96	0.38	4.75
300 mm	185.7	1358	439.1	0.39	4.05

Based on the results of the FE model using ABAQUS, the calibrated model was utilized to do parametric studies with the objective of investigating the effects of the slab thickness, the tensile reinforcement ratio, the compressive reinforcement ratio and the slab axial load level on the behavior of the RC flat slabs under static loading. All RC flat slabs tested in this parametric study had the same plan dimensions, reinforcement arrangement, boundary conditions, concrete and steel material properties as specimen CS40-3 that mentioned before.

##### 4.1 Effects of slab thickness

Specimens with slab thickness changing from 105 mm to 300 mm were tested and the compression and tension longitudinal reinforcement ratios were kept 0.35% and 2.2% respectively. Fig. 6 shows the load-deflection curves for these slabs. It is clear that increasing the slab thickness produced a higher load carrying capacity and reduced the ultimate displacement. All slabs failed by punching shear. The cone of punching shear at ultimate load is shown in Fig. 7. The numerical results showed that increasing the slab thickness did not change the punching failure mode of the RC flat slab with high reinforcement ratios.

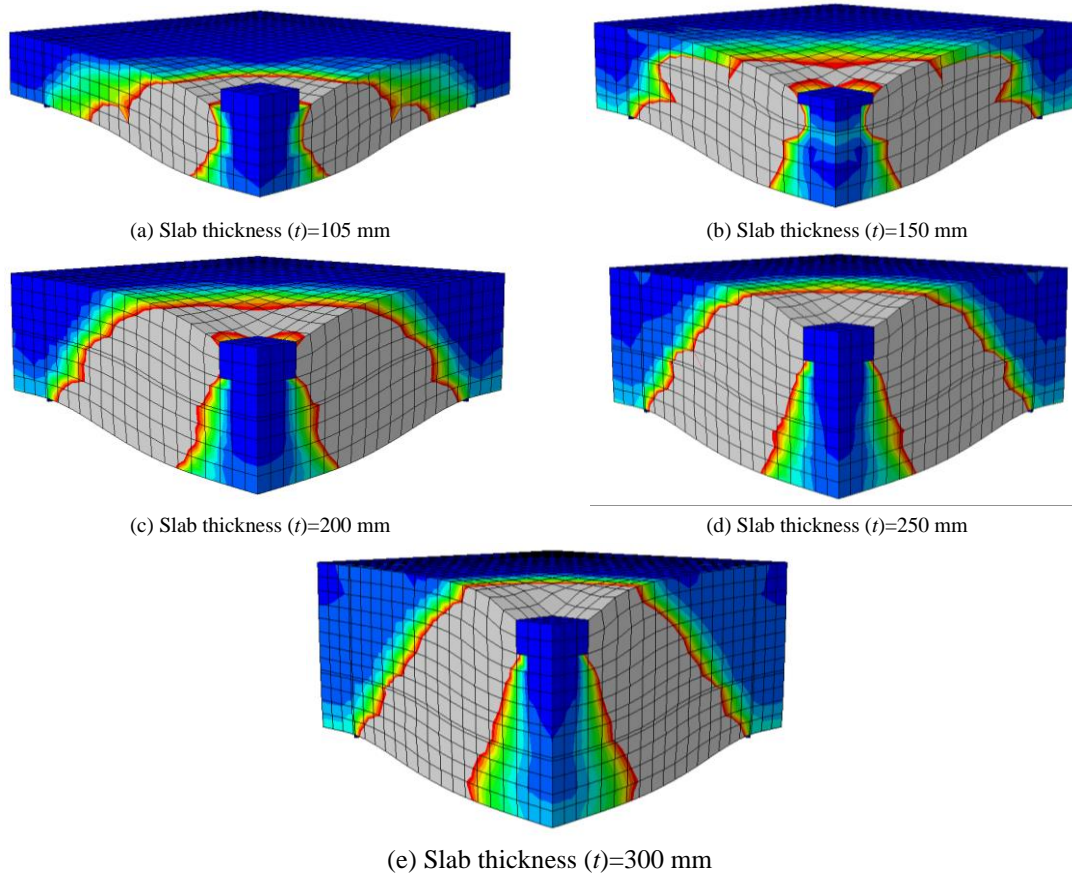


Fig. 7 Concrete failure mechanisms for specimens with different slab thicknesses ( $t$ )

Table 4 shows the influence of the slab thickness on the shear resistance of RC flat slab. It illustrates that because the normalized loads  $V/(\sqrt{f_c} \cdot b_0 \cdot d)$  nearly coincide, the strength developed approximately proportional to the normalization parameter  $b_0 d$ . Where  $b_0$  was a control perimeter set at  $d/2$  of the border of the support region,  $d$  was the effective depth of the slab and  $f_c$  was the compressive strength of concrete. According to the ACI318-14 (2014), the normalized punching load at critical section must be less than 0.33. Table 4 shows that the maximum value of normalized load was 0.39. This value is higher than the value recommended by ACI318-14. Results showed that for RC flat slabs with high reinforcement ratios as the thickness increased, the ultimate punching load ( $V_u$ ) increased as listed in Table 4. The ultimate deflection ( $\Delta_u$ ) of slabs decreased observably with increasing the thickness, as shown in Table 4.

#### 4.2 Effects of flexural reinforcement

The yield line theory is an efficient tool to estimate the ultimate flexural strength of a reinforced concrete slab. It gives the failure load that produces flexural failure ( $V_f$ ) in terms of the bending moment  $M$  per unit width of the slab at yielding of the flexural reinforcement. The value of  $M$  is almost linearly dependent on the flexural reinforcement ratio ( $\rho$ ). In absence of shear reinforcement, slabs with relatively small  $\rho$  fail in flexural mode when  $V_f < V_c$ , where  $V_c$  is the nominal shear strength provided by concrete.

When  $\rho$  is high such that  $V_f > V_c$ , the failure mode is punching.

To show the effect of tension and compressive reinforcement on the punching shear behavior of flat slab structures, slabs with 105 mm thickness and with various reinforcement ratios were simulated.

##### 4.2.1 Tensile reinforcing steel

The effect of the percentage of tensile flexural reinforcement was studied by simulating slabs with different percentages:  $\rho=0.3\%$ ,  $0.55\%$ ,  $0.65\%$ ,  $0.75\%$ ,  $0.86\%$ ,  $1.24\%$ ,  $2.2\%$ , and  $2.78\%$  respectively. All slabs had a compression flexural reinforcement ratio of  $0.35\%$ . The corresponding response curves are shown in Fig. 8. It was found that the percentage of the reinforcement had a significant effect on the punching strength of the slabs. As the percentage of the reinforcement increased, the ultimate load of the slab increased but the corresponding ductility decreased. Also, the mode of failure changed from flexural failure to punching shear failure with increasing the tensile flexural reinforcement, as listed in Table 5.

It is noted that the slabs with  $\rho=0.75\%$ ,  $0.86\%$ ,  $1.24\%$ ,  $2.2\%$ , and  $2.78\%$  failed by punching failure while the slabs with  $\rho=0.30\%$ ,  $0.55\%$  and  $0.65\%$ , failed by flexural failure. In other words, the RC flat slabs that were reinforced by a tensile reinforcement ratio more than  $0.65\%$  failed by punching failure. In order to investigate the influence of the tension reinforcement ratio on the punching response, the relation between the normalized punching load and tensile

Table 5 Numerical results for slabs with various tensile reinforcement ratios

Tensile reinforcement ratio	$V_u$ (kN)	$V_u/(\sqrt{f_c} \cdot b_o \cdot d)$	Failure mode
0.3%	121.9	0.187	Flexural failure
0.55%	169.4	0.260	Flexural failure
0.65%	185.1	0.284	Flexural failure
0.75%	198.7	0.305	Punching failure
0.86%	207.6	0.318	Punching failure
1.24%	227.6	0.349	Punching failure
2.2%	251.9	0.386	Punching failure
2.78%	259.6	0.398	Punching failure

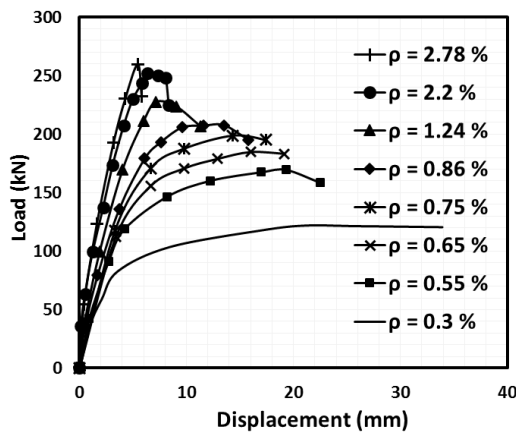


Fig. 8 Load-deflection curves of slabs with different tensile reinforcement ratios

reinforcement ratio was studied for these slabs and presented in Fig. 9 and Table 5. It is clearly that the ratio of the tensile reinforcement had a considerable influence on the slab punching shear strength. As the percentage of tensile reinforcement increased, the punching load increased but the ductility of the slabs decreased. Such effect was not included in ACI 318-14. According to Fig. 9, it is clearly shown that if the tensile reinforcement ratio of the RC flat slab decreased about 0.98%, the normalized punching load exceeded recommended value of 0.33. Fig.10 shows the concrete failure mechanisms and the steel plastic strain distributions for the slabs with different tensile reinforcement ratios. It was found that the plastic strain width at the bottom face of the slab (the shear crack) decreased when the tensile reinforcement ratio increased.

4.2.2 Compressive reinforcing steel

Slabs with various compressive reinforcement ratios as 0.30%, 0.55%, 0.86%, 1.24%, 1.68%, and 2.20% were selected and simulated. The tensile reinforcement ratio for all slabs was kept constant at 2.2%. Fig. 11 shows the load-deflection curves of the slabs with different ratios of compressive reinforcement. The results showed that increasing the percentage of compressive reinforcement enhanced the ultimate load of the slab but the mode of failure did not changed about the punching failure for all slabs. The effect of the compression steel on the punching shear resistance are shown in Fig. 12 and Table 6. It was noticed that by increasing the percentage of the compressive

Table 6 Numerical results for the slabs with different compressive reinforcement ratios

Compressive reinforcement ratio	$V_u$ (kN)	$V_u/(\sqrt{f_c} \cdot b_o \cdot d)$	Failure mode
0.30%	251.9	0.386	Punching failure
0.55%	252.1	0.387	Punching failure
0.86%	256.75	0.394	Punching failure
1.24%	260.25	0.399	Punching failure
1.68%	270.57	0.415	Punching failure
2.20%	290.2	0.445	Punching failure

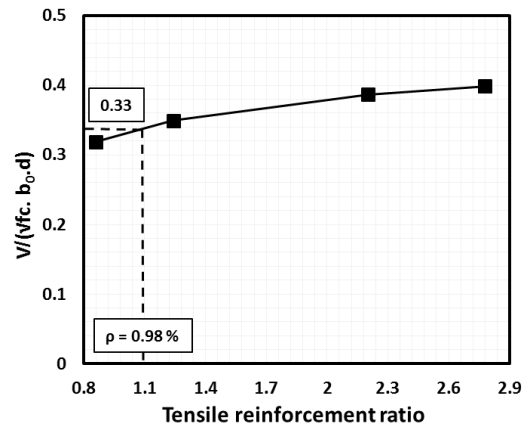


Fig. 9 The relation between normalized punching load and tensile reinforcement ratio

reinforcing steel, the punching load enhanced more than increasing the ratio of the tensile reinforcement. The maximum value of the normalized load reached 0.44 at the compressive reinforcement ratio of 2.20% as listed in Table 6.

4.3 Effects of compressive diaphragm action (axial load level)

The main function of RC flat slab systems can be classified into two structural roles. The first is supporting the gravity loads and transferring these loads to the vertical elements such as the columns. The second role is to connect all vertical elements together at each floor level and transferring the lateral loads to different lateral-load-resisting elements, such as frames and shear walls. The last action is called the diaphragm action, in which, the slab suffers from axial and bending stresses.

To investigate the effect of the axial load level on the punching shear behavior of the RC flat slabs, three RC slabs with dimensions and mechanical properties similar to specimen CS40-3 were studied. All other parameters were kept constant but with different values of axial load levels:  $n=0\%$ ,  $20\%$  and  $40\%$ . Where  $n=P_s/(f_c \cdot A_g)$  \*One side gross area of the slab \*100 and  $P_s$  is the slab axial load and exist in the  $X$  and  $Y$  directions. The numerical load-displacement curves for these slabs are shown in Fig. 13. After testing the slab models, it is clear that all specimens behaved similarly in the linear stage. However, there were obvious stiffness differences among these curves in the nonlinear stage.

All slabs failed by punching failure. Fig. 13 indicate that

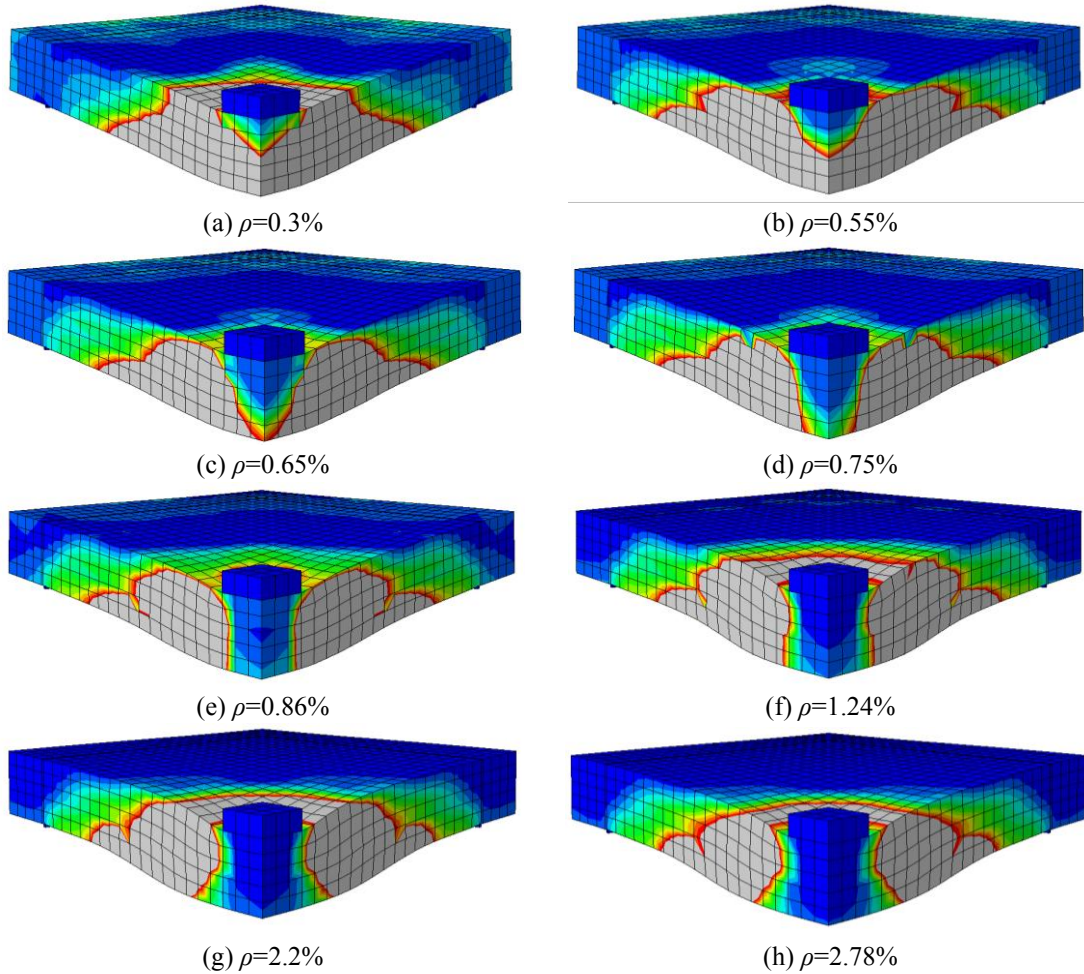


Fig. 10 Concrete failure mechanisms for specimens with different tensile reinforcement ratios

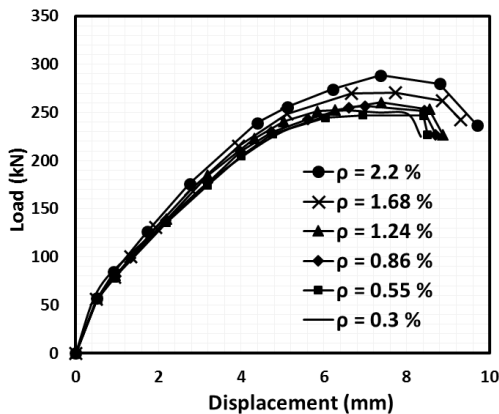


Fig. 11 Load-deflection curves of the slabs with different ratios of compressive reinforcement

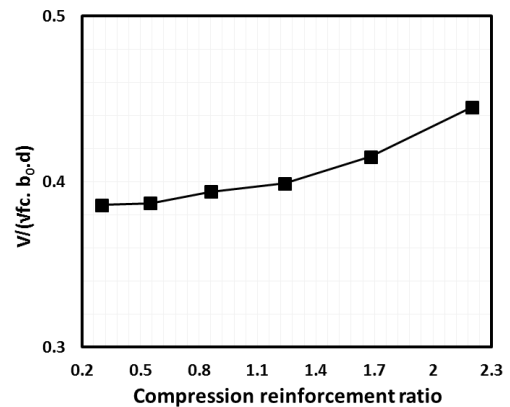


Fig. 12 The relation between normalized punching load and compressive reinforcement ratio

when the axial load level reached 20%, the ultimate punching load increased by 5% ( $V_u=264.9$  kN) compared to the slab without an axial load ( $V_u=251.9$  kN).

The axial force on the slab generated strain concentrations in the punching cone area as shown in Fig. 14. The analysis outcomes highlighted the potentially unconservative effects of neglecting the actual varying axial load demand when assessing the behavior of the RC flat slab system.

It is emphasized that in order to obtain the actual behavior of RC flat slab, accounting for the variation of the axial load on slabs should be used. After finishing the numerical investigation using ABAQUS, the effects of all parameters on the punching capacity of the slabs was summarized in Fig. 15. It was noticed that the slab thickness had the highest effect on the punching behaviour of the RC flat slabs.

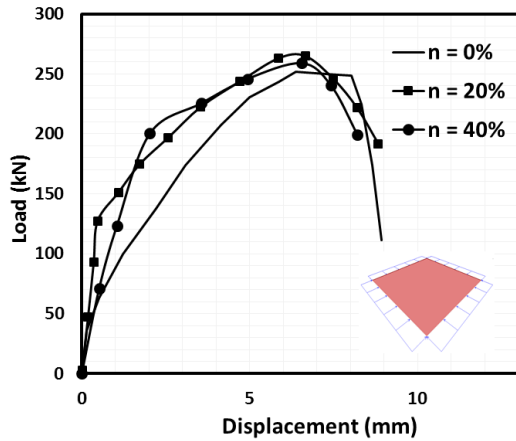


Fig. 13 Load-deflection curves of the slabs subjected to different levels of axial compression load

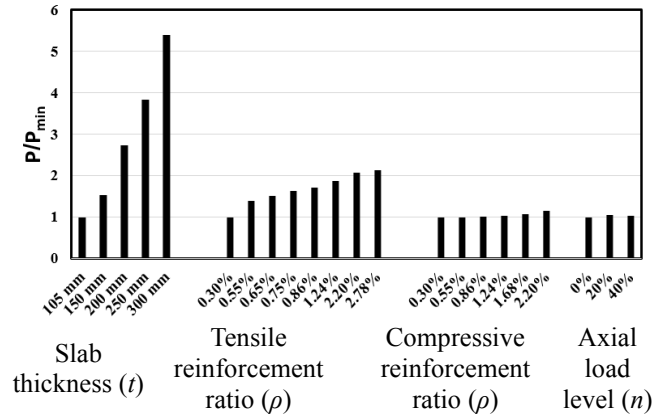


Fig. 15 Effect of the different parameters on the punching capacity of the slabs

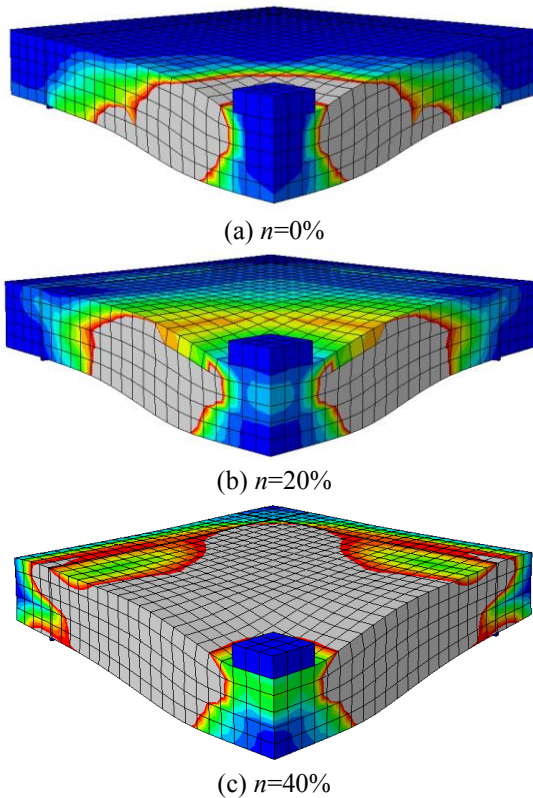


Fig. 14 Failure mechanisms for specimens with different axial load levels

### 5. Simplified model using SAP2000

In order to reduce the burden on the modelling and to expand the study, a simplified model using SAP2000 program (2017) was developed. A nonlinear layered four-nodes quadrilateral shell element was used to simulate the nonlinear flexural behavior of the RC flat slab. The mechanical properties of the concrete and the reinforcing steel either in the elastic stage or in the inelastic stage were defined. The behavior of this element depended on the concepts of the mechanics of composite material. This element consisted of a number of layers in order to separate

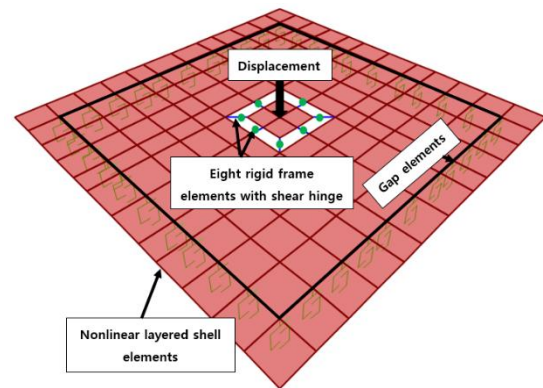


Fig. 16 Boundary conditions and loading used in SAP2000

the modelling of the concrete and the steel. The axial strain and curvature of the middle layer were observed and the strains and the curvatures of the other layers were calculated according to the assumption that plane remains plane. The corresponding stress was evaluated through the constitutive relations of the material assigned to the layer. The previous observations showed that the structural performance of the RC flat slabs can be directly connected to the material constitutive law. The constitutive model of the rebar was set as the elastic with a hardening plasticity model while the stress-strain curve of the concrete was presented by Mander (1988).

The inelastic punching shear behavior of the RC flat slab plays a dominant role in the prediction of the slab performance. For this purpose, eight shear hinges were inserted in eight rigid frame elements located at  $(d/2)$  from the column face and used to tie the two parts of the slab (The first part of slab was inside the punching critical section and connected to the column while the other part was located outside the punching critical section). The model is shown in Fig. 16. The force-displacement relationships were defined and assigned for each shear hinge to model the brittle failure of punching shear of concrete, which were obtained from the ABAQUS results. Without using these shear hinges, the punching shear failure will not be captured and the flexural failure mode will be dominant. The gap elements available in the SAP2000 program were used to simulate the interaction between the

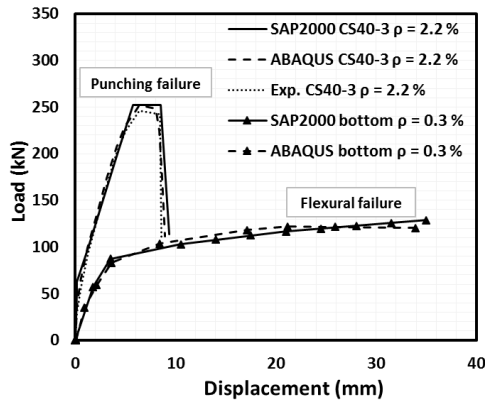


Fig. 17 Load-deflection curves of slab CS40-3 with bottom reinforcement ratios 2.2% and 0.3%

concrete surface and the supports.

Nonlinear static pushover analysis was carried out. In the nonlinear static pushover procedure, a monotonically increase of the forces were applied to a nonlinear mathematical model of the structure until the displacement of the control node exceeded the target displacement.

Two RC flat slabs were used as a verifications for this simplified model and compared with the ABAQUS results. The first slab was the control specimen considered in the current study (CS40-3) while the second slab was identical to CS40-3 but with a bottom reinforcement ratio of 0.3% in

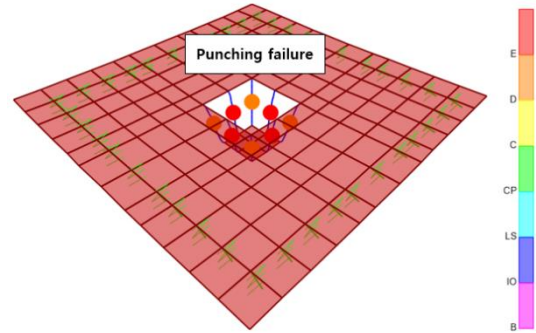
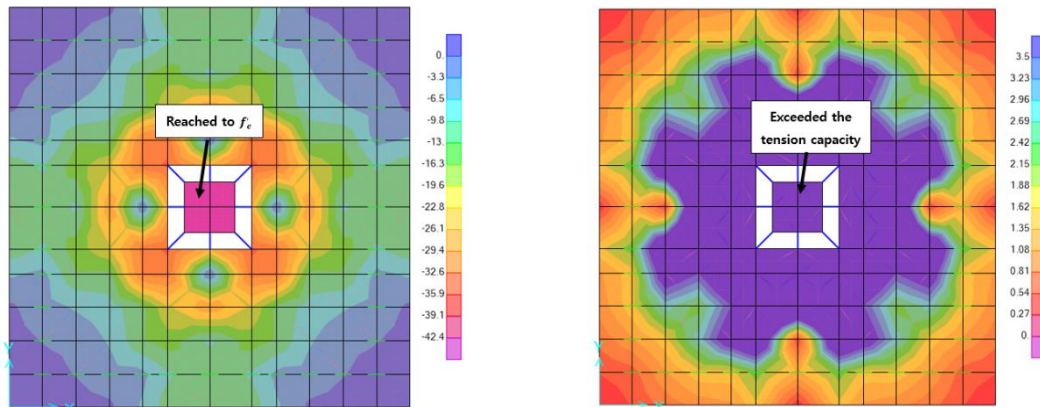


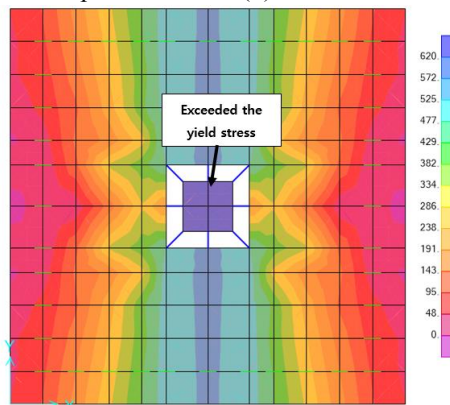
Fig. 18 Punching failure of slab CS40-3 with bottom reinforcement ratio 2.2%

each direction. Note that these two slabs were analysed before using ABAQUS (see in Fig. 4 and Fig. 8).

Fig. 17 shows the load-displacement curves for these two slabs resulting from the simplified model and the ABAQUS. The results confirmed that the proposed simplified model was able to predict quiet well the response of the RC flat slab subjected to static loading. Also, the failure modes for the two slabs using the simplified model were similar to the failure modes that were obtained from the ABAQUS. The slab CS40-3 failed under the punching shear failure (See in Fig. 18) while the other slab failed by flexural ductile failure (See in Fig. 19). The performance level of an immediate occupancy (IO), life safety (LS) and

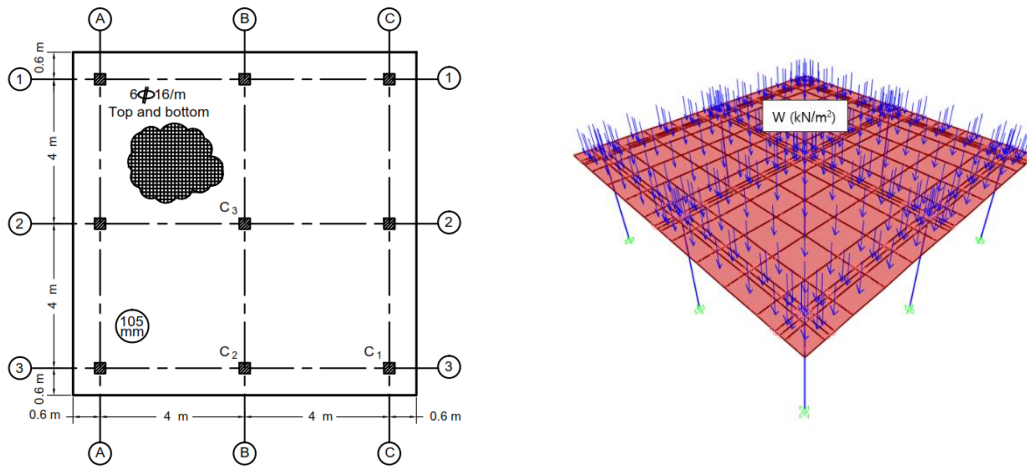


(a) Minimum shell layer stresses at top fiber of slab (b) Maximum shell layer stresses at bottom fiber of slab



(c) S11 shell layer stresses for reinforcement of X direction at bottom of slab

Fig. 19 Flexural failure of slab CS40-3 with bottom reinforcement ratio 0.3%



(a) Geometric and reinforcement details of the slabs (b) Boundary conditions and loads used in SAP2000

Fig. 20 Details of the structure used in the case study used in SAP2000

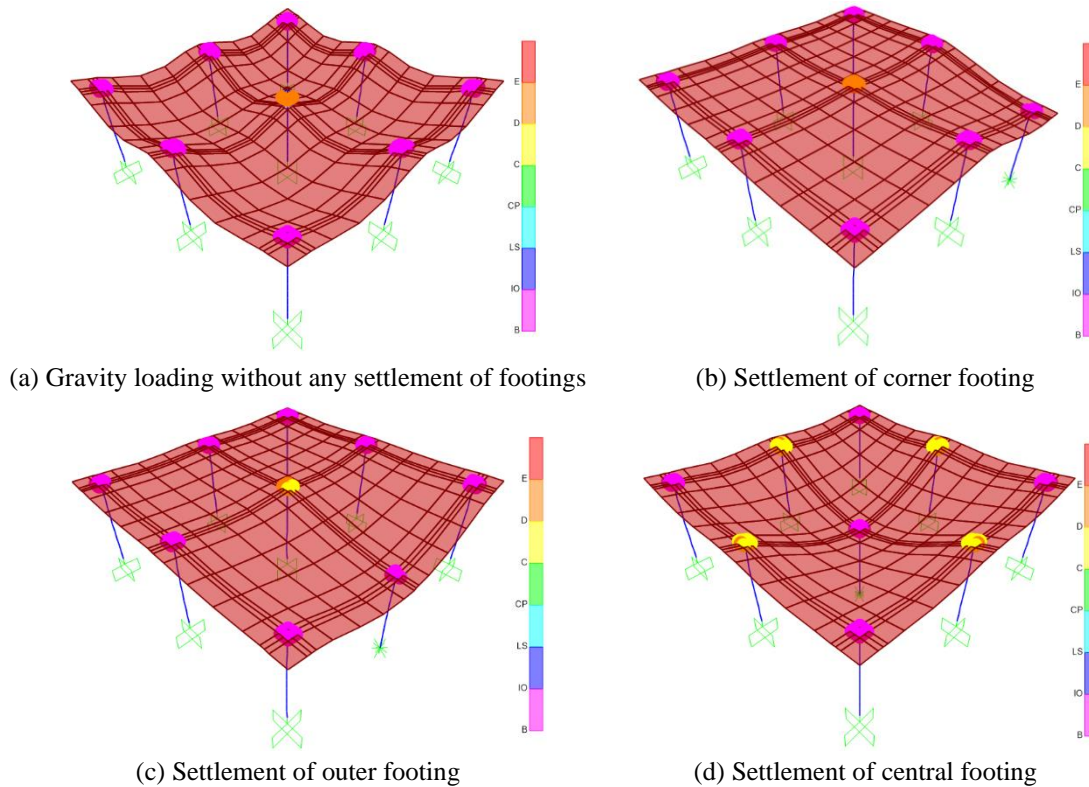


Fig. 21 SAP2000 failure mechanisms for structures used in case study

collapse prevention (CP) were discussed in FEMA-356 (2000).

### 6. Case study

To show the effects of the footings settlement on the behavior of the RC flat slabs, a flat slab system with dimensions and details, as shown in Fig. 20, was modelled using the aforementioned simplified model. In addition, P-M2-M3 and shear hinges were assigned at the column ends to capture the flexural or the shear failures of the columns. P-M2-M3 means plastic hinges take into account the

interaction between the axial force and the flexural moments on the column section. The top and bottom reinforcement of RC flat slabs were 6Ø16/m in both directions. The thickness of the slabs was 105 mm. all RC columns had the same dimensions of 300×300 mm and their height was 3.0 m. The longitudinal reinforcement of the columns was 9Ø16 with 7Ø8/m as transverse stirrups. The mechanical properties of the concrete and the reinforcement shown in Fig. 3 were used in this case study.

The main aim of this case study was studying the footings settlement whether the corner or the outer or the central footing. The three footings C1, C2, and C3, were chosen in this study as shown in Fig. 20(a). The control

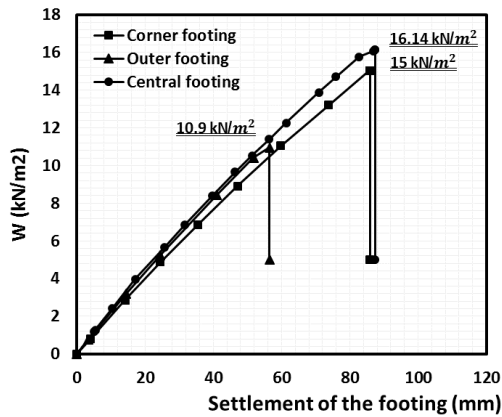


Fig. 22 Relationship between footing settlement and the carrying loads for the different cases of the slabs

structure, without a settlement of any footing, was found to fail at the ultimate surface load ( $W_u$ ) of 15.5 kN/m<sup>2</sup> and the punching shear failure of the slab above the central column was the dominant failure mechanism, as illustrated in Fig. 21(a). Where  $W_u$  was defined as the loads acting on the square meter at the top surface of the slab that represented the gravity loads.

It was found that when the corner footing (C1) or the central footing (C3) settled, the ultimate surface loads of slabs ( $W_u$ ) were 15 kN/m<sup>2</sup> and 16.4 kN/m<sup>2</sup> respectively. The position of the punching shear failure moved from above the central column to above the four outer columns (See Fig. 21(b) to Fig. 21(d)). Finally, in case of the outer footing settlement (C2), the ultimate surface load of the slabs reduced to 10.9 kN/m<sup>2</sup>. That means that the settlement of the outer footings in the RC flat slab framed systems may reduce the ultimate gravity load carrying capacity by 30% and the punching failure formed above the central column. No P-M2-M3 plastic hinges were observed at the column ends, this means that the punching shear failure of the slab is the dominant failure mechanism. Fig. 22 shows the slab surface load and settlement curves for the various cases of the footings settlement.

## 7. Conclusions

This research investigated the punching shear behavior of RC flat slabs considering the effects of thickness, horizontal reinforcement, axial load level and footings settlement. The following conclusions are drawn from numerical simulations:

- The proposed finite element models either using the ABAQUS or the SAP2000 could give a quite accurate prediction for the behavior of RC flat slabs, including the carrying capacity, the monotonic curves and varies probable failure modes. It proved the rationality of the selected element types, constitutive models and contact models comparing the experimental results. The finite element model provided a strong tool for studying the performance of RC flat slabs.
- The flexural tension and compression reinforcement ratios had a considerable effect on the slab punching

shear resistance. With increasing the percentage of reinforcement, the value of the punching load increased.

- With increasing the percentage of the compressive reinforcement, the punching load increased more greatly than when increasing the ratio of the tensile reinforcement. The slabs with a compressive reinforcement ratio of 2.49% achieved the maximum value of the normalized load which reached 0.44.
- The slab axial load (The diaphragm action) affects the behavior of RC flat slabs by changing their peak loads.
- The settlement of the outer footings in RC flat slab framed structures may reduce the ultimate gravity load carrying capacity by 30% while the settlement of the central footings moves the position of punching shear failure from above the central column to above the outer columns.

## References

- Abaqus Theory Manual (6.14) (2014), Dassault Systemes, Providence, RI, USA.
- ACI Committee & International Organization for Standardization (2008), Building Code Requirements for Structural Concrete (ACI 318-08) and Commentary, American Concrete Institute.
- Ahsan, R. and Zahura, F.T. (2017), "Numerical study on effect of integrity reinforcement on punching shear of flat plate", *Comput. Concrete*, **20**(6), 731-738. <https://doi.org/10.12989/cac.2017.20.6.731>.
- Alam, A.J., Amanat, K.M. and Seraj, S.M. (2009), "An experimental study on punching shear behavior of concrete slabs", *Adv. Struct. Eng.*, **12**(2), 257-265. <https://doi.org/10.1260/136943309788251650>.
- American Concrete Institute. (2014), Building Code Requirements for Structural Concrete (ACI 318-14), Commentary on Building Code Requirements for Structural Concrete (ACI 318R-14), An ACI Report, American Concrete Institute, ACI.
- Anna Polak, M. (2005), "Shell finite element analysis of RC plates supported on columns for punching shear and flexure", *Eng. Comput.*, **22**(4), 409-428. <https://doi.org/10.1108/02644400510598750>.
- Belletti, B., Walraven, J.C. and Trapani, F. (2015), "Evaluation of compressive membrane action effects on punching shear resistance of reinforced concrete slabs", *Eng. Struct.*, **95**, 25-39. <https://doi.org/10.1016/j.engstruct.2015.03.043>.
- Birkle, G. and Dilger, W.H. (2008), "Influence of slab thickness on punching shear strength", *ACI Struct. J.*, **105**(2), 180.
- Einpaal, J., Bujnak, J., Fernández Ruiz, M. and Muttoni, A. (2016), "Study on influence of column size and slab slenderness on punching strength", *ACI Struct. J.*, **113**, 135-145.
- Eurocode 2; BS EN 1992-1-1 (2004), Design of Concrete Structures, General Rules and Rules for Buildings, Section 3.1.5.
- Federal Emergency Management Agency (2000), Pre-Standard and Commentary for Seismic Rehabilitation of Buildings, Report No. FEMA-356, Washington DC.
- Genikomsou, A.S. and Polak, M.A. (2014), "Finite element analysis of a reinforced concrete slab-column connection using ABAQUS", *Structure Congress ASCE*, **813**, 823. <https://doi.org/10.1061/9780784413357.072>.
- Guan, H. (2009), "Prediction of punching shear failure behaviour of slab-edge column connections with varying opening and column parameters", *Adv. Struct. Eng.*, **12**(1), 19-36. <https://doi.org/10.1260/136943309787522605>.
- Guandalini, S., Burdet, O. and Muttoni, A. (2009), "Punching tests of slabs with low reinforcement ratios", *ACI Struct.*, **106**(1), 87-95.

- Lips, S., Fernández Ruiz, M. and Muttoni, A. (2012), "Experimental investigation on punching strength and deformation capacity of shear-reinforced slabs", *ACI Struct. J.*, **109**, 889-900.
- Mander, J.B., Priestley, M.J. and Park, R. (1988), "Theoretical stress-strain model for confined concrete", *J. Struct. Eng.*, **114**(8), 1804-1826. [https://doi.org/10.1061/\(ASCE\)0733-9445\(1988\)114:8\(1804\)](https://doi.org/10.1061/(ASCE)0733-9445(1988)114:8(1804)).
- Meisami, M.H., Mostofinejad, D. and Nakamura, H. (2013), "Punching shear strengthening of two-way flat slabs using CFRP rods", *Compos. Struct.*, **99**, 112-122. <https://doi.org/10.1016/j.compstruct.2012.11.028>.
- Sagaseta, J., Muttoni, A., Fernández Ruiz, M. and Tassinari, L. (2011), "Non-axis-symmetrical punching shear around internal columns of RC slabs without transverse reinforcement", *Mag. Concrete Res.*, **63**(6), 441-457. <https://doi.org/10.1680/mac.10.00098>.
- Saleh, H., Kalfat, R., Abdouka, K. and Al-Mahaidi, R. (2018), "Experimental and numerical study into the punching shear strengthening of RC flat slabs using post-installed steel bolts", *Constr. Build. Mater.*, **188**, 28-39. <https://doi.org/10.1016/j.conbuildmat.2018.08.064>.
- SAP 2000. Version 20 (2017), CSI-Computers and Structures Inc., 2000.
- Schmidt, P., Kueres, D. and Hegger, J. (2019), "Punching shear behavior of reinforced concrete flat slabs with a varying amount of shear reinforcement", *Struct. Concrete*, **21**(1), 235-246. <https://doi.org/10.1002/suco.201900017>.
- Shu, J., Plos, M., Zandi, K., Johansson, M. and Nilenius, F. (2016), "Prediction of punching behaviour of RC slabs using continuum non-linear FE analysis", *Eng. Struct.*, **125**, 15-25. <https://doi.org/10.1016/j.engstruct.2016.06.044>.